Supporting Information

In-situ synthesis of rosette-like Co-doped FeNiOOH/NF for seawater oxidation

Mingyuan Shi[a,b], Tianmi Tang[b], Liyuan Xiao[b], Jingyi Han[b], Xue Bai[b], Yuhang Sun[a,b], Yuanyuan Ma[a,*], and Jingqi Guan[b,*]

[a] College of Chemistry and Chemical Engineering, Qiqihar University, Heilongjiang Province 161006, China. *E-mail: mayuanyuan1219@126.com (Y.Y. Ma)

[b] Institute of Physical Chemistry, College of Chemistry, Jilin University, 2519 Jiefang Road, Changchun 130021, P. R. China. *E-mail: guanjq@jlu.edu.cn (J.Q. Guan)

Synthesis of Co_x-FeNiOOH/NF

Nickel foam (2 cm × 2 cm) was treated in 3 M HCl, distilled water and absolute ethanol for 15 min, respectively. Then, $Co(NO_3)_2 \cdot 6H_2O$ (0, 0.1, 0.2, 0.4 and 0.6 mmol), 2 mmol $Fe(NO_3)_3 \cdot 9H_2O$, 2 mmol $Ni(NO_3)_2 \cdot 6H_2O$, 0.24 g NH_2CONH_2 and 0.075 g PVP were dissolved in 20 mL of H_2O via ultrasonic treatment. Afterwards, the mixture was transferred into a 25 mL Teflon-lined stainless steel autoclave, and a piece of NF was inserted, which was heated at 100 °C for 12 hours. After natural cooling, the in situ grown NF was washed several times with distilled water and ethanol and dried at 60 °C for 12 h. After drying, the synthesized sample was named Co_x-FeNiOOH/NF, where x is the molar content of Co.

Characterization

Powder X-ray diffraction (XRD) patterns were collected using a Shimadzu XRD-6000 with CuKα radiation (40 kV, 30 mA). SEM images were recorded on a HITACHI SU8020 field emission scanning electron microscope. Raman spectra were acquired using a Renishaw micro-Raman spectrometer with a 532 nm laser at 0.2 mW. The valence state was determined using XPS recorded on a Thermo ESCALAB 250Xi. The X-ray source selected was monochromatized Al Kα source (15 kV, 10.8 mA). Region scans were collected using a 30 eV pass energy. Peak positions were calibrated relative to C 1s peak position at 284.6 eV.

Electrochemical measurements

All electrochemical measurements were performed on a CHI760E electrochemical working station at room temperature. The catalysts were measured in 1.0 M KOH aqueous solution using a typical three-electrode configuration. Linear sweep voltammetry (LSV) polarization curves were acquired at a scan rate of 5 $mV \cdot s^{-1}$. Electrochemical impedance spectroscopy (EIS) measurements were performed at open-circuit potential in the frequency range from 100 kHz to 0.1 Hz with an a.c. perturbation of 5 mV. All potentials measured were calibrated to RHE using the following equation: E (versus RHE) = E (versus SCE) + 0.241 V + 0.0591 pH.

The Faradaic efficiency was calculated using the equations:

$$FE = (V/V_m)\, e\, N_A\, Z/Q$$

where V is the volume of gas (L), V_m is the standard molar volume (22.4 L mol^{-1}), e is the electron charge (1.6×10^{-19}), N_A is the Avogadro number (6.02×10^{23}),

Z is the number of electrons needed to form O_2 molecular (for O_2, Z = 4), and Q is the amount of power consumed during electrolysis (C).

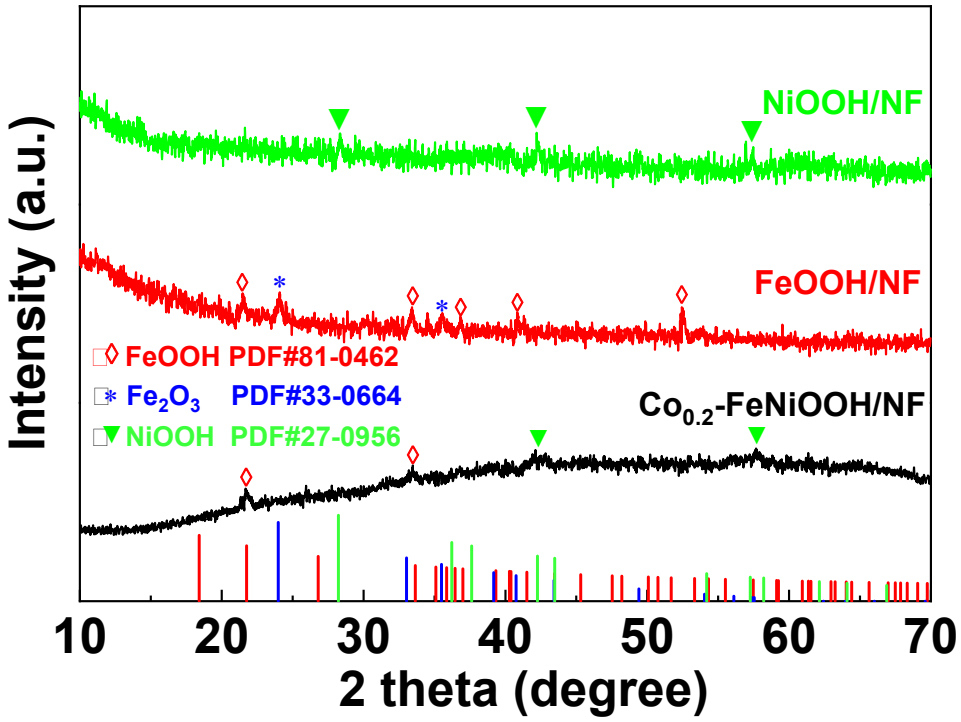

Fig. S1. XRD patterns of NiOOH/NF, FeOOH/NF and $Co_{0.2}$-FeNiOOH/NF.

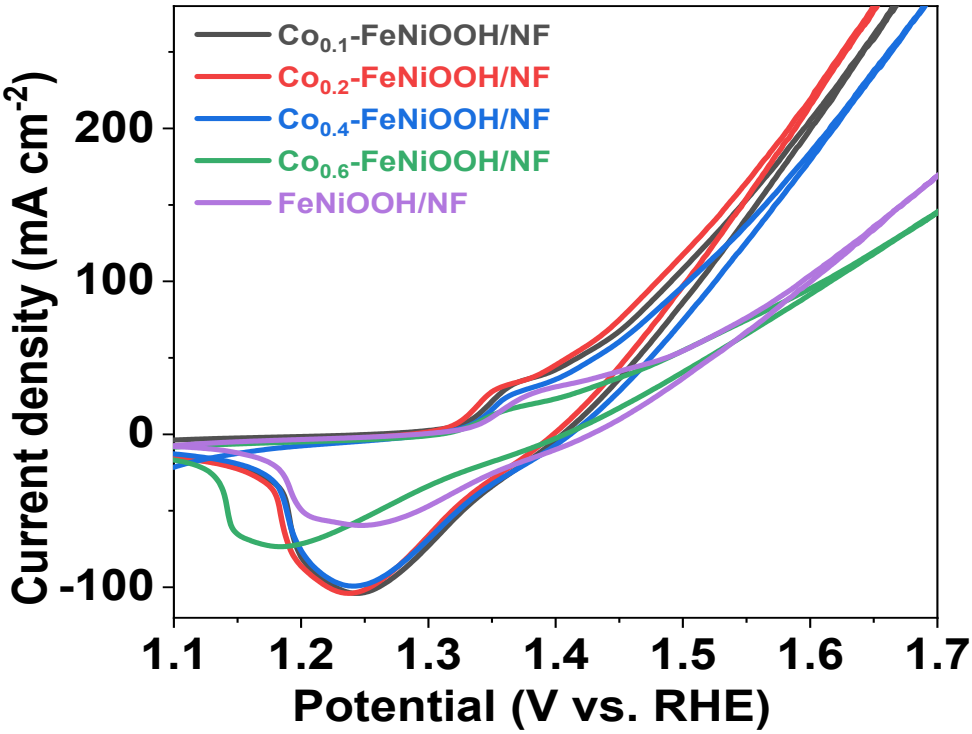

Fig. S2. CV curves of $Co_{0.1}$-FeNiOOH/NF, $Co_{0.2}$-FeNiOOH/NF, $Co_{0.4}$-FeNiOOH/NF, $Co_{0.6}$-FeNiOOH/NF and FeNiOOH/NF at a scan rate of 5 mV/s.

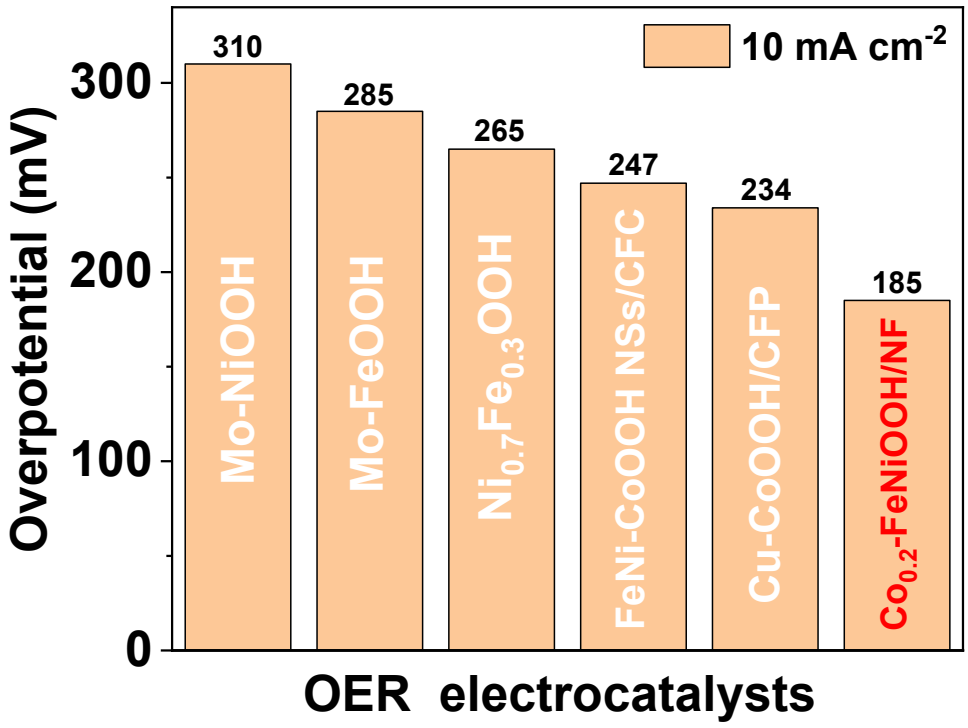

Fig. S3. Overpotential comparison at 10 mA cm^{-2}.

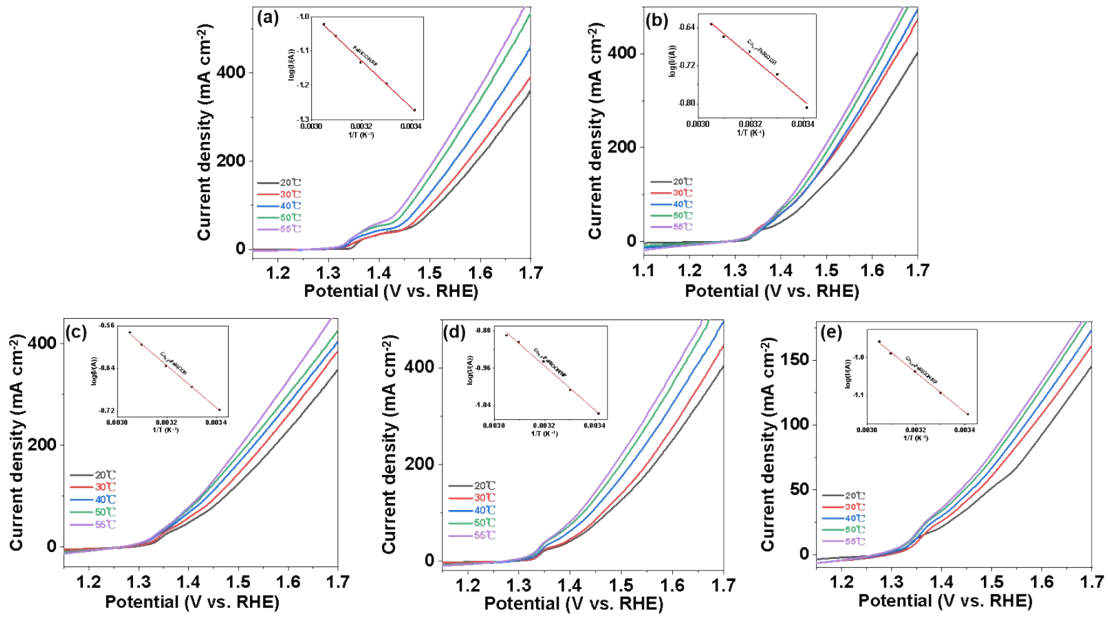

Fig. S4. OER polarization curves of FeNiOOH/NF, $Co_{0.1}$-FeNiOOH/NF, $Co_{0.2}$-FeNiOOH/NF, $Co_{0.4}$-FeNiOOH/NF and $Co_{0.6}$-FeNiOOH/NF in three-electrode configuration in 1 M KOH at 20 °C, 30 °C, 40 °C, 50 °C and 55 °C.

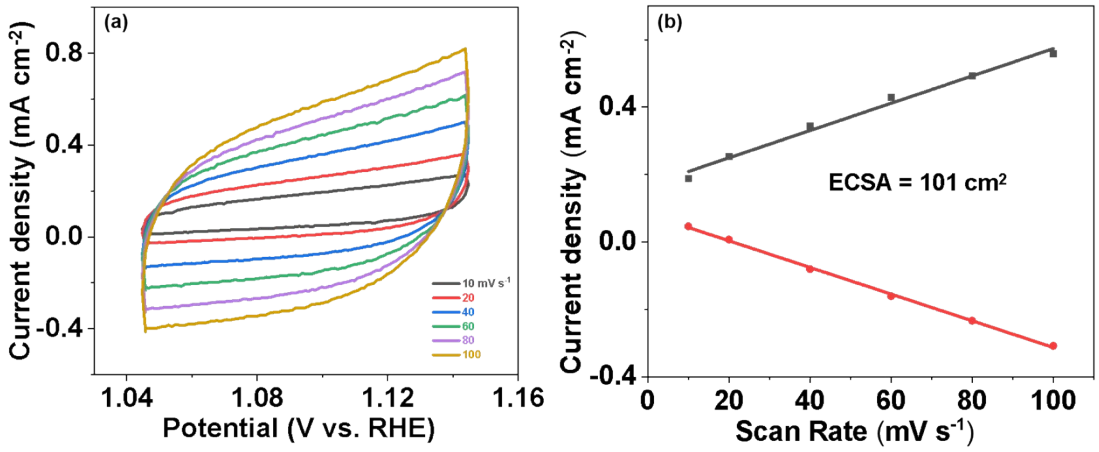

Fig. S5. (a) CVs of the $Co_{0.2}$-FeNiOOH/NF measured in a non-Faradaic region at different scan rate. (b) The cathodic and anodic currents measured as a function of the scan rate.

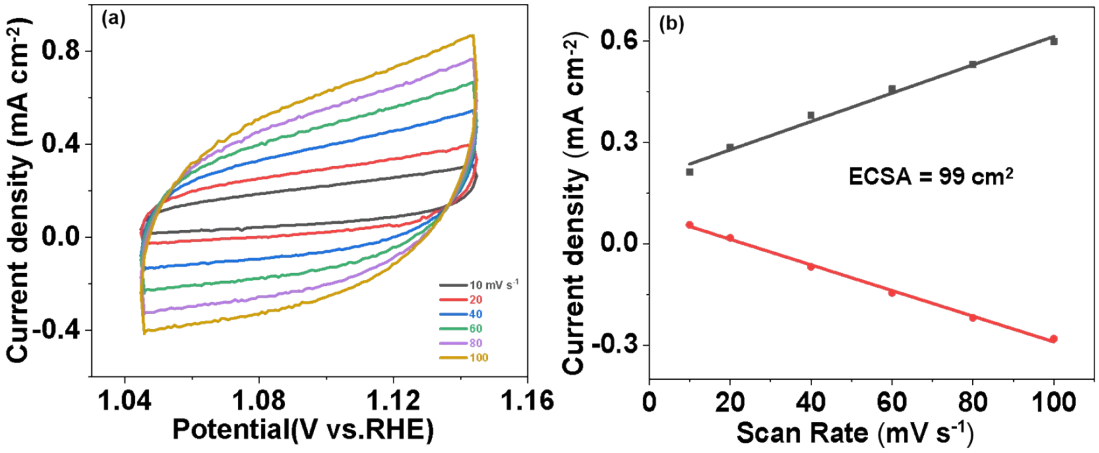

Fig. S6. (a) CVs of the $Co_{0.1}$-FeNiOOH/NF measured in a non-Faradaic region at different scan rate. (b) The cathodic and anodic currents measured as a function of the scan rate.

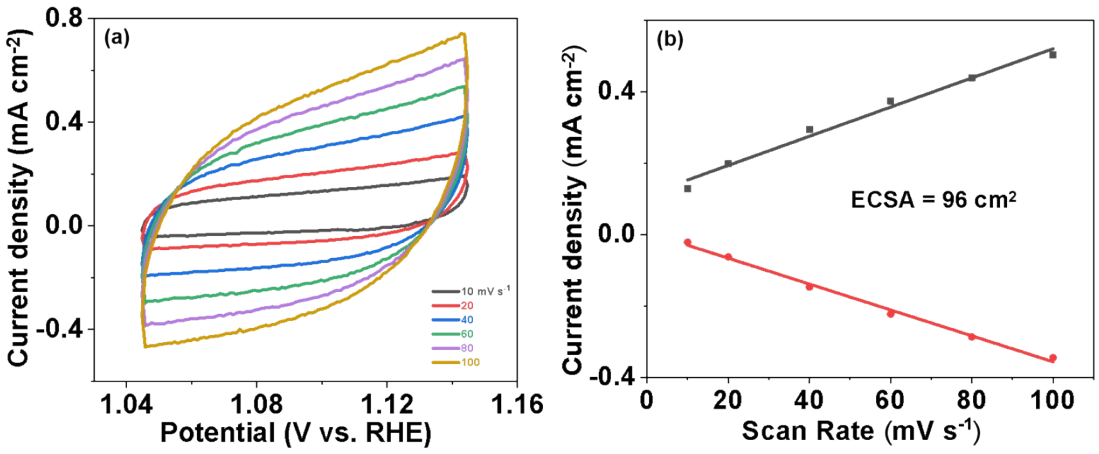

Fig. S7. (a) CVs of the $Co_{0.4}$-FeNiOOH/NF measured in a non-Faradaic region at different scan rate. (b) The cathodic and anodic currents measured as a function of the scan rate.

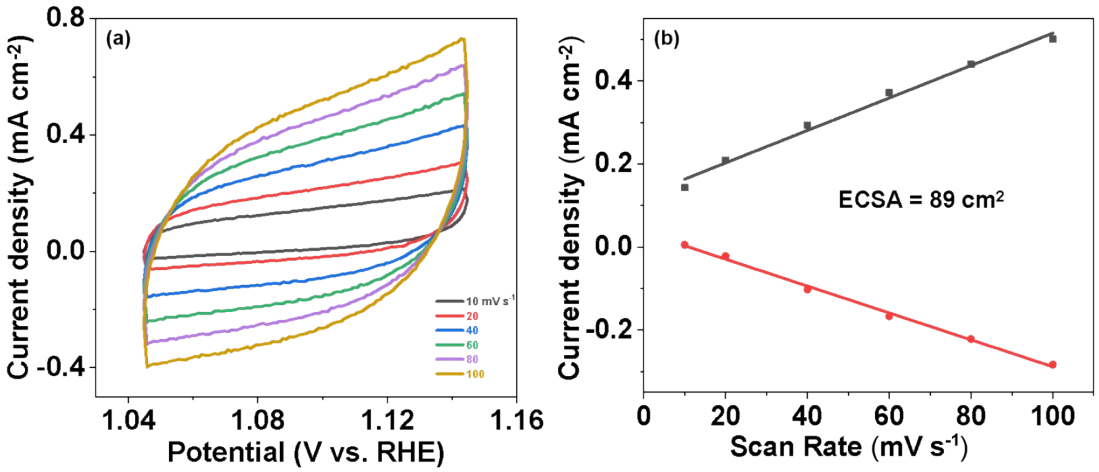

Fig. S8. (a) CVs of the $Co_{0.6}$-FeNiOOH/NF measured in a non-Faradaic region at different scan rate. (b) The cathodic and anodic currents measured as a function of the scan rate.

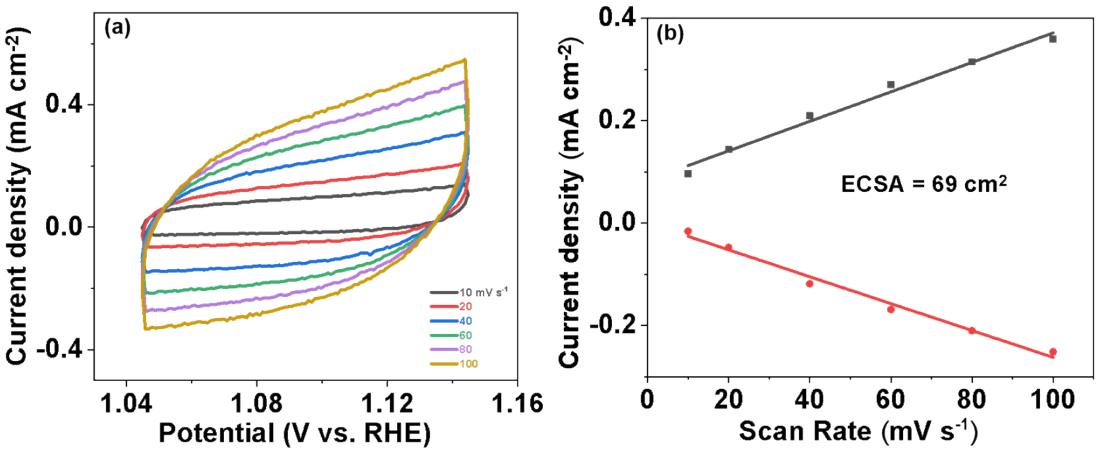

Fig. S9. (a) CVs of the FeNiOOH/NF measured in a non-Faradaic region at different scan rate. (b) The cathodic and anodic currents measured as a function of the scan rate.

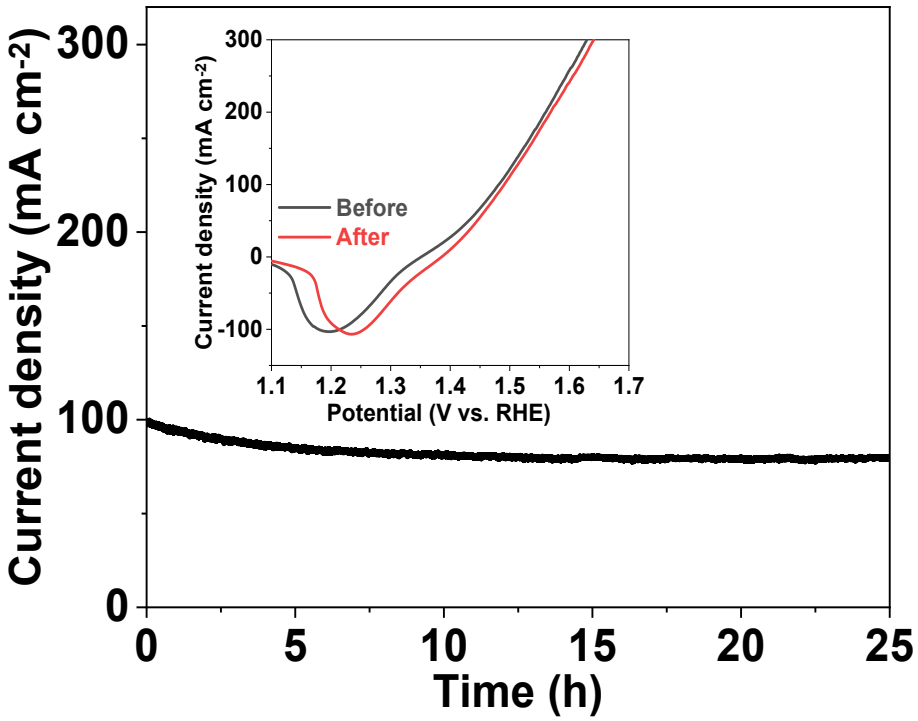

Fig. S10. Chronoamperometric curve of the $Co_{0.2}$-FeNiOOH/NF in 1 M KOH.

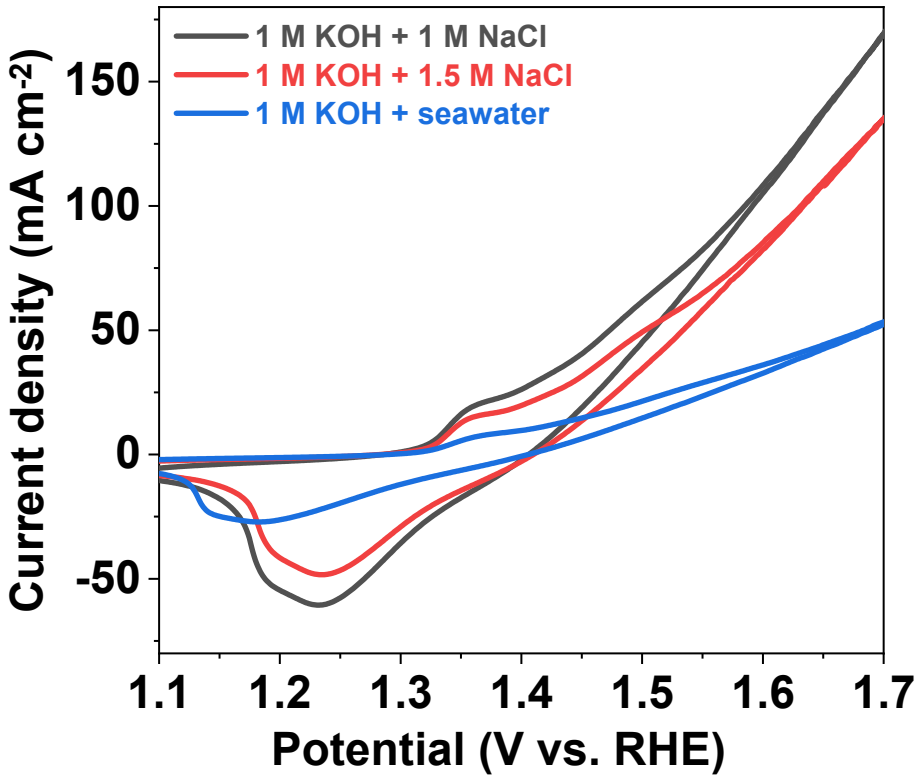

Fig. S11. CV curves of $Co_{0.2}$-FeNiOOH/NF in different electrolytes at 5 mV/s.

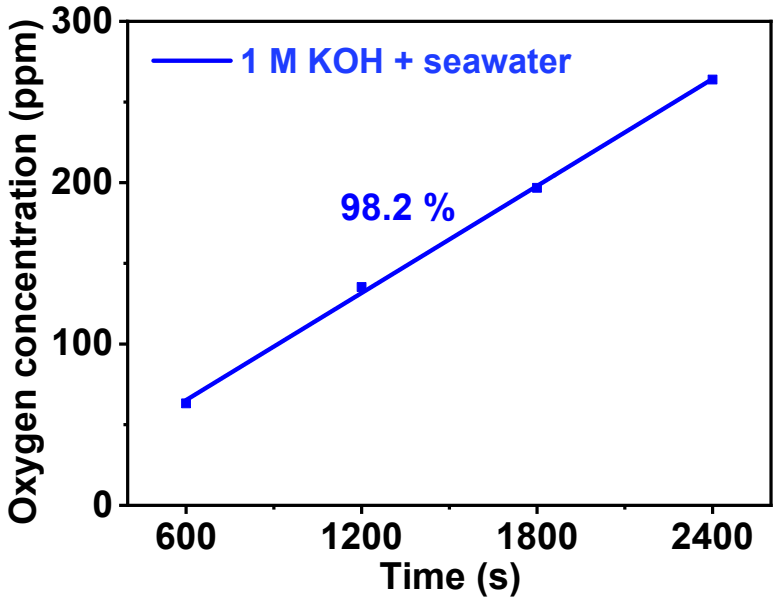

Fig. S12. Faraday efficiency of $Co_{0.2}$-FeNiOOH/NF in 1 M KOH + seawater at 10 mA cm^{-2}.

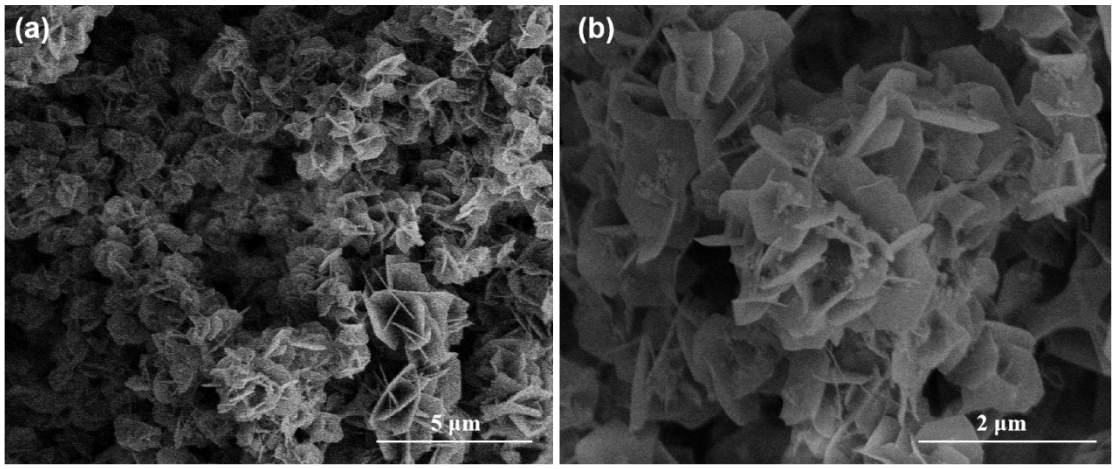

Fig. S13. (a, b) SEM images of $Co_{0.2}$-FeNiOOH/NF after OER testing.

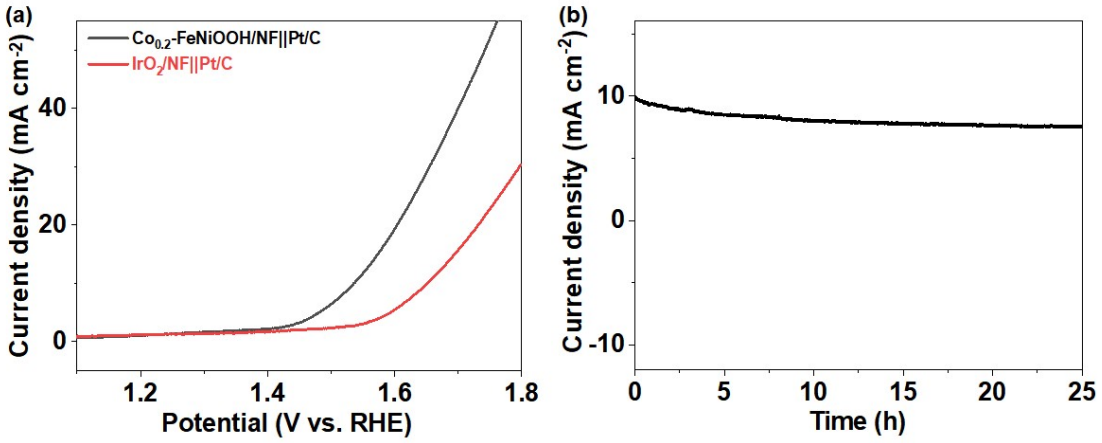

Fig. S14. (a) LSV curves of $Co_{0.2}$-FeNiOOH/NF||Pt/C and IrO_2/NF||Pt/C in overall water splitting. (b) Stability test.